Journal of Applied Polymer Science

# Synthesis and architecture study of a reactive polybutadiene polyamine as a toughening agent for epoxy resin

**Hossein Abdollahi, Ali Salimi, Mehdi Barikani**
Iran Polymer and Petrochemical Institute, Post Office Box 14975-112, Tehran, Iran
Correspondence to: A. Salimi (E-mail: A.Salimi@ippi.ac.ir)

**ABSTRACT:** In this study, a novel reactive toughener for the epoxy resin was developed and compared with traditional hydroxyl-terminated polybutadiene (HTPB). For this purpose, the highly reactive aliphatic amine-terminated polybutadiene (ATPB) was synthesized at ambient conditions by nucleophilic substitution amination. The characterizations of the product were provided by Fourier transform infrared and $^1$H NMR spectroscopy. According to the mechanical test results, incorporation of ATPB into epoxy networks can significantly toughen the epoxy matrix. The addition of 10 phr ATPB increased the critical stress intensity factor ($K_{IC}$) and critical strain energy release rate ($G_{IC}$) of the epoxy from 0.85 to 2.16 MPa $m^{1/2}$ and from 0.38 to 3.02 kJ $m^{-2}$, respectively. Furthermore, unlike HTPB, the presence of the ATPB did not deteriorate the tensile strength of the matrix. The toughening and failure mechanisms were discussed based on the epoxy network morphological characteristics. The reduction in crosslinking density and glass transition temperature of the epoxy system upon modification with liquid rubbers was confirmed by dynamic mechanical analysis. This article opens up the possibility of utilizing reactive flexible diamines with polybutadiene backbone as effective toughening agents for thermoset polymers. © 2016 Wiley Periodicals, Inc. J. Appl. Polym. Sci. **2016**, *133*, 44061.

**KEYWORDS:** mechanical properties; polyolefins; synthesis and processing; thermosets

Received 3 March 2016; accepted 1 June 2016
**DOI: 10.1002/app.44061**

## INTRODUCTION

As one of the most important polymers, the epoxy resins have drawn much attention due to their excellent mechanical properties, high adhesiveness to different substrates in addition to superior heat and chemical resistance. These resins are widely used as matrix resins in high performance applications such as the structural adhesives,[1] coatings,[2] composite materials,[3] microelectronic encapsulants,[4] and as skin binding in surgical incisions.[5] However, their high crosslinking density often leads to undesirable properties such as brittleness and low fracture toughness.

The rigidity and strength are desired properties for most engineering applications, whereas the low resistance of crack growth or resin brittleness restricts the wide applications of epoxies. Therefore, toughening of epoxies has been a challenging issue for decades. Several techniques introduced for improving toughness of the epoxy resins that could be classified in two categories of physical modification (addition of a toughening agent into the epoxy network)[6–8] and chemical modification of the epoxy structure.[9,10] Some common toughening agents in the polymeric systems are liquid elastomers,[6] inorganic particles,[7,11] and thermoplastics.[8] However, they impair some final properties of the resin. On the contrary, modification of chemical structure could improve the physical properties.[12]

As the most common toughening agent, the incorporation of liquid rubber into the epoxy causes an increase in fracture toughness with reduction in glass transition temperature ($T_g$) and modulus.[13,14] Copolymer of acrylonitrile and butadiene with end carboxyl functional groups (CTBN) has been used as one of the efficient toughening agents.[13,15] This copolymer is able to react with epoxide groups. However, the only way to synthesize carboxyl terminated oligomers is bulk polymerization, which is difficult to be controlled.[16] Another category is the hydroxyl-terminated polybutadienes (HTPBs). The immiscibility of HTPB with epoxy resin causes phase separation during curing reactions. The reactivity and selectivity of the rubber play important role in achieving the proper toughening. The presence of functional groups in the rubber chain can promote the formation of chemical bonds with epoxy matrix. These chemical bonds lead to efficient stress transfer between rubber moieties and the matrix.[17]

In order to improve the compatibility between epoxy matrix and HTPB rubber particles, the HTPBs must be chemically bonded to the matrix. The functionalization of HTPB has been reported by chemical modification of the unsaturated bonds in

the polymer backbone or hydroxyl end groups to different form such as epoxidized-HTPB (E-HTPB),[18] isocynate-terminated polybutadiene (NCOTPB),[19] and carboxyl-terminated polybutadiene (CTPB).[19] However, an effective adhesion between the phases is difficult to be achieved due to low reactivity of E-HTPB, low reaction rates of CTPB and low required functionality (i.e., hydroxyl groups) of the liquid DGEBA for reaction with NCOTPB. To obtain reactive HTPB, the amination of HTPB has been reported in few studies.[20,21] Chao *et al.*[20] synthesized an amine-terminated polybutadiene (ATPB) by cyanoalkylation of the HTPB by Michael addition of acrylonitrile in the presence of a base, followed by hydrogenation. However, the ATPB is hydrogenated (either prior to or after the amination reaction) to saturate polymer. Kar and Banthia[21] prepared an ATPB by Fischer esterification of HTPB with *p*-amino benzoic acid, which can toughen DGEBA. However, reported ATPB had aromatic amine that has lower reactivity than aliphatic type and high temperature (200 °C) was needed to perform modification of epoxy. Also, synthesis process required relatively harsh conditions.

Among different modification methods, the amination of HTPB could be a reliable method mainly due to high tendency of amines to react with epoxy groups. The amines are derivatives of ammonia which are classified as aromatic, alicyclic, and aliphatic. Aliphatic amines perform suitable cure at room temperature with excellent all-around properties.[22] Besides, to the best of our knowledge, the nucleophilic substitution process has not been used for amination of HTPB, and the effect of aliphatic ATPB on toughness and mechanical properties of the epoxy resin has not been reported before.

The aim of our study is to introduce a mild condition synthesis of ATPB as a polybutadiene polyamine with end aliphatic amine functional groups. The efficiency of ATPB for toughness improvement of a DGEBA-type epoxy resin will be evaluated through morphological and mechanical properties. There is also a comparative study using HTPB to better elucidate the effect of phase architecture on the final properties of epoxy network.

## EXPERIMENTAL

### Materials

The diglycidyl ether of bisphenol A; DGEBA under the trade name EPON 828 from USA with a viscosity of 13 Pa s (at 25 °C) was used. The epoxide equivalent weight; EEW, was calculated 191 g/eq as determined through acid titration. The curing agent was diethylenetriamine (DETA; ≥99%, amine value = 1626 mg KOH/g), which was purchased from Sigma Aldrich, Buchs, Switzerland. The HTPB with an average molecular weight of 3000 g/mol and a viscosity of 8 Pa s (at 25 °C) was obtained from Bayer Material Science, Leverkusen, Germany. The chemical reagents were benzene sulfonyl chloride (BSC; 98%; Merck, Darmstadt, Germany), triethylamine (TEA; 99%; Merck), hexamethylenediamine (HMDA; 98%; Sigma Aldrich). All the reagents were synthesis grade and used as received. Methanol (99%), heptane (≥99%), chloroform (99%), and toluene (≥99.5%) were purchased from Merck and used as solvent without further purification.

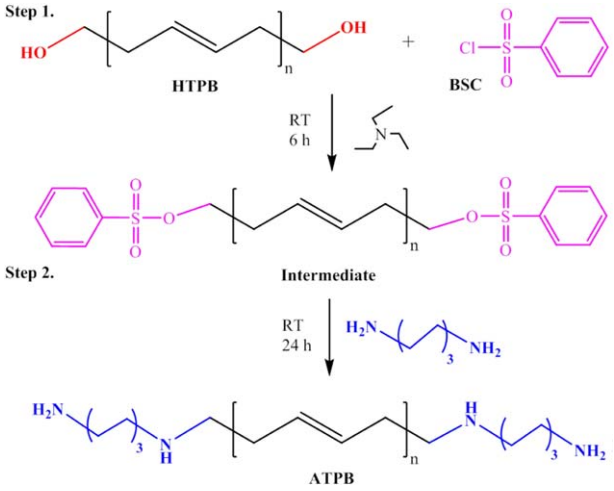


**Figure 1.** Schematic representation of the synthesis of ATPB. [Color figure can be viewed in the online issue, which is available at wileyonlinelibrary.com.]

### Synthesis of the ATPB

ATPB was synthesized by sequence of nucleophilic substitution reactions in two steps. In the first step, the HTPB (15 g, 10 mmol OH) was dissolved in dry toluene (100 mL). Then, BSC (1.2 eq, 2.12 g, 12 mmol) was added to the solution and stirred under a nitrogen blanket. Then, TEA (1.2 eq, 1.22 g, 12 mmol) was added and reaction mixture left at room temperature with constant stirring for 6 h (Figure 1, step 1). The intermediate was poured into the heptane (50 mL), filtration was done, and the solvent was removed from the filtrate by rotary evaporation.

In the second step, the intermediate was added dropwise to the solution of HMDA (10 eq, 11.6 mL, 0.1 mol) in chloroform (50 mL) and was stirred at room temperature for 24 h (Figure 1, step 2). Then, the solvent was removed by rotary evaporation. In both steps, purification was done by washing of the products with methanol.

### Preparation of the Rubber-Modified Epoxy

The epoxy resin was modified using individual HTPB and ATPB liquid rubbers with different amounts, that is, 5, 10, and 15 phr based on total epoxy resin. The liquid ATPB was totally added into epoxy resin for about 12 h through continuous stirring at room temperature. Then, the required stoichiometric amount of the hardener DETA (20.1 g/eq of epoxy group) was added and mixed completely. In order to remove the bubbles from bulk of the modified resins, the mixtures were agitated and subsequently degassed under vacuum for about 15 min. The samples were poured into silicone molds and cured at 25 °C for 24 h followed by post curing at 75 °C for 6 h.

All the samples were encoded using ER for epoxy resin, H for HTPB, and A for ATPB. The number in each code denotes for the amount of rubber in phr based on total epoxy resin. In the case of ATPB-modified epoxy, because of the presence of amine groups in ATPB, the equal amount of ATPB amine was subtracted from the amount of required curing agent (i.e., DETA).

### Characterization

Fourier transform infrared (FTIR) spectra were obtained from a Bruker (IFS 484; Bruker, Rheinstetten, Germany) spectrometer. By using deuterated CF at room temperature, the whole $^1$H NMR spectra were recorded in a Bruker (Avance 400 MHz NMR) spectrometer.

The morphological properties of fractured surface of samples were investigated by scanning electron microscopy (SEM; VEGA\\TESCAN; Vega SEM, Tescan Company, Brno, Czech Republic) at an accelerating voltage of 15 kV. After the tensile test, the fractured surfaces of samples were first etched using toluene to extract the rubber phase. The etched surfaces were then dried under vacuum and coated with a thin layer of gold. To analyze SEM images, JMicroVision software was used. Therefore, the number ($D_n$) and volume ($D_v$) average diameters and polydispersity of the HTPB particles were calculated using following equations:

$$D_n = \frac{\sum n_i D_i}{\sum n_i} \quad (1)$$

$$D_v = \frac{\sum n_i D_i^4}{\sum n_i D_i^3} \quad (2)$$

$$PD = \frac{D_v}{D_n} \quad (3)$$

where $n_i$ is number of the liquid rubber droplets having a diameter of $D_i$.

The dynamic mechanical analysis (DMA) was performed in a dynamic mechanical analyzer (TRITEC 2000 DMA; Triton, Nuneaton, England) using the three-point bending mode. The tests were carried out at a frequency of 1 Hz and a temperature sweep from −100 to 200 °C with a 5 °C min$^{-1}$ scan rate. The displacement and strain employed for the temperature sweep were 0.01 mm and 0.03%, respectively. The dimensions of the sample were 2 × 10 × 30 mm$^3$. Besides, the crosslinking density ($v$) and molecular weight between two crosslinks ($M_c$) of the cured neat and modified epoxies were determined from DMA results.

For measurement of the density of the samples, a Kern (Kern & Sohn GmbH company, Germany) Model 770 balance (densitometer) was used with an accuracy of $\pm 10^{-4}$ g.

### Mechanical Testing

The tensile tests were performed in a universal testing machine (STM 20; Santam, Tehran, Iran) according to ASTM D-638 at a crosshead speed of 4 mm min$^{-1}$ [nominal strain rate was about 0.15 mm (mm min)$^{-1}$]. Type V specimens with thickness of 2 mm were prepared for tensile properties, and the calculated elastic modulus ($E$) was used in critical strain energy release rate equation. The values were obtained from average of at least five specimens.

Flexural tests were also performed with rectangular samples according to ASTM D-790 using a Santam STM 20 testing machine via crosshead speed of 1.3 mm min$^{-1}$ [rate of straining of the outer fiber was considered as 0.01 mm (mm min)$^{-1}$]. The dimensions of the samples were 120 × 13 × 3 mm$^3$ using a length span of 48 mm. The values were obtained from average of at least five specimens.

Fracture toughness was taken in to account to evaluate toughness of samples according to ASTM D-5045 by Santam STM 20 testing machine at a crosshead speed of 10 mm min$^{-1}$. The single edge notch samples with dimensions of 40 × 8 × 4 mm$^3$ were tested for fracture toughness, using the notch depth of 4 mm and a length span of 32 mm. The fracture toughness was evaluated in terms of the critical stress-intensity factor ($K_{IC}$) and critical strain energy release rate ($G_{IC}$) that calculated using the following equations:

$$K_{IC} = \frac{P}{BW^{1/2}} f(x) \quad (4)$$

$$f(x) = 6\sqrt{x}\frac{[1.99 - x(1-x)(2.15 - 3.93x + 2.7x^2)]}{(1+2x)(1-x)^{3/2}} \quad (5)$$

$$G_{IC} = \frac{(K_{IC})^2}{E} \quad (6)$$

where $P$ is the load at the crack initiation; $B$ is the thickness of the sample; $W$ is the sample width; $a$ is the crack length and $x = a/w$. The values were obtained from average of at least five specimens.

## RESULTS AND DISCUSSIONS

### FTIR and NMR Characterization of ATPB

The formation of ATPB was first investigated through FTIR spectra. The FTIR spectra of HMDA and HTPB in addition to ATPB are shown in Figure 2(a–c), respectively. As shown in Figure 2(a), the spectrum of HMDA showed a broad band at 3300 cm$^{-1}$ that is assigned to the stretching vibration of different N–H. The other characteristic absorption bands of the HMDA, which is the amine source in amination, appeared at 727, 1320, and 1571 cm$^{-1}$. The peak at 727 cm$^{-1}$ is attributed to the bending motion associated with four or more $CH_2$ groups in the open chain (called a long-chain band) of the HMDA, the 1320 cm$^{-1}$ band is due to C—N stretch vibrations and 1571 cm$^{-1}$ attributed to the H—N bending vibration.[23] The spectrum of HTPB in Figure 2(b) showed a peak at 3410 cm$^{-1}$ which is due to O—H stretching, in addition to the peaks at 1640 and 3072 cm$^{-1}$ corresponding to C═C and =C—H stretching vibrations. The out-of-plane bending of the =C—H groups occurred in the range 650–1000 cm$^{-1}$.[23] Therefore, the peaks at 723 and 912 and 966 cm$^{-1}$ indicate the presence of *cis*, *vinyl*, and *trans* conformations of the =C–H group. As shown in Figure 2(c) for ATPB, the additional peak at 3361 cm$^{-1}$ maybe due to the presence of N—H stretching of amine functional group. Besides, there are main peaks at 1569 cm$^{-1}$, which is due to N–H bending vibration and at 1319 cm$^{-1}$ due to C–N stretching as a mark of C–$NH_2$ and C–NH–C.[23] Note that these peaks were not in the spectrum of HTPB. A comparison of the spectra indicates the successful formation and purification of the ATPB during amination through nucleophilic substitution reactions in the mild condition.

The curing reaction of epoxy resin with amine groups of ATPB (using the stoichiometric proportion of the epoxy and ATPB) was monitored in FTIR analysis. The IR spectra of ATPB, neat epoxy, and epoxy cured with ATPB are shown in Figure 2(c–e), respectively. The comparison between spectra showed that the chemical linkages were formed during the curing process. The

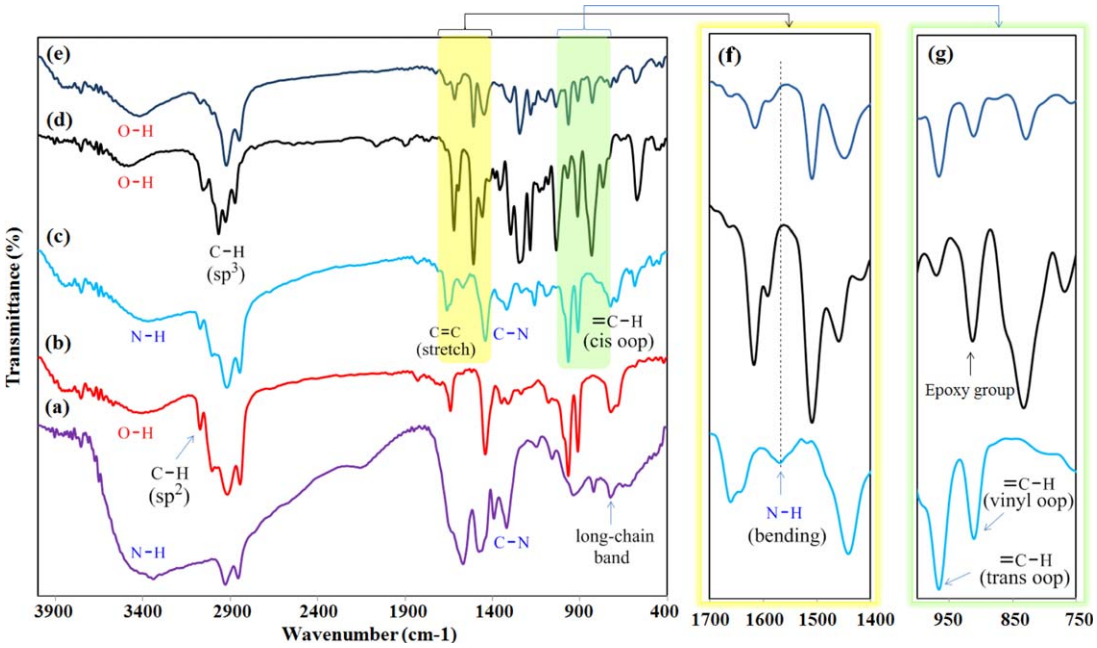


**Figure 2.** FTIR spectra of (a) HMDA, (b) HTPB, (c) ATPB, (d) neat DGEBA, and (e) DGEBA cured with ATPB. Inset of the curves c–e in the range of (f) 1400–1700 $cm^{-1}$ and (g) 750–1000 $cm^{-1}$. [Color figure can be viewed in the online issue, which is available at wileyonlinelibrary.com.]

chemical reactions between epoxy ring and amine functional groups of ATPB leads to disappearance of the peaks related to the amine and epoxy groups. Since there is no characteristic peaks of the amine (at 1569 and 3361 $cm^{-1}$) and epoxy (at 914 $cm^{-1}$) groups in the cured epoxy spectrum [Figure 2(e)], it may be concluded that all epoxy groups of the resin were reacted with amine groups of the ATPB. Therefore, the reactivity of this kind of ATPB is higher than that of reported before in Ref. 21.

The NMR spectroscopy analysis was used for more precise characterization of the synthesized liquid rubbers and evaluation of the ATPB. As shown in Figure 1, the first synthetic step was the introduction of the terminal benzene sulfonate ($BSO^-$, as a good leaving group) on the HTPB. In order to convert the available hydroxyl groups of HTPB to the activated form with a leaving group, they were reacted with BSC at a mild condition. The NMR spectra of the HTPB, intermediate and ATPB are shown in Figure 3. The peaks at around 1.3, 2, 5, and 5.4 ppm are prominent peaks that are due to the protons of polybutadiene backbone. In addition to these peaks, the $^1H$ NMR spectrum of HTPB in Figure 3(a) shows the main peak at 4.1 ppm corresponding to hydroxyl (—$CH_2$—OH) protons. As it can be seen in Figure 3(b) for the spectrum of intermediate, the main peak related to the hydroxyl group was eliminated, while the signals of aromatic ring protons are appeared between 7.63–8.07 ppm. Therefore, it can be concluded that the synthesis of the intermediate was carried out completely. In the second step, the HMDA was used as an amine source for amination of the prepared intermediate. In Figure 3(c) for the spectrum of the ATPB, the appearance of the additional peaks at about 1.4 and 2.5 ppm maybe attributed to the presence of the HMDA structure. The disappearance of the aromatic ring proton signals supports the formation of ATPB and indicates good separation in the absence of any impurities and side products.

The existence of double bond in polybutadiene based rubbers is one of the inherent properties; so that the measurement of unsaturation degree seems necessary during the amination process. Therefore, the NMR spectroscopy analysis was used to determine the degree of unsaturation. The degree of unsaturation was evaluated from the following equation[24]:

$$\text{Unsaturation degree } (\%) = \frac{4(c+e)+8(f)}{2(x)+3(c+e)+4(f)} \times 100 \qquad (7)$$

where $c$ and $e$ are the peak area of the methine (—CH) protons in olefin region, and $f$ attributed to methylene (—$CH_2$) ones. Also, $x$ is the summation of all the peak area of the protons in the aliphatic region as shown in Figure 3(a). The calculations suggested the same amount of unsaturation "90%" for the primary ($c = 4.83$, $e = 0.93$, $f = 1.73$, and $x = 8.2$) and intermediate ($c = 26.92$, $e = 3.33$, $f = 9.57$, and $x = 45.08$) materials. For the final product, the peaks related to HMDA protons overlap the peaks of aliphatic protons of rubber. Therefore, eq. (7) is not useful for the calculation of unsaturation degree for the final product. But, because the area ratio of the peak related to olefinic rubber protons to its aliphatic protons ($c/b$ ratio) is the same as two previous spectra (about 0.6), it can be concluded that the double bonds were not changed in the final product. The results state that the reaction conditions and the chemical agents are not potentially able to change the unsaturation degree of the rubber, maybe due to the reaction under mild conditions.

Consequently, the FTIR and NMR results showed that the amination route for preparing of ATPB had significant advantages such as milder reaction condition, easier purification process and modification of epoxy resins than previously reported article.[21] Furthermore, in comparison with literature,[20,21] the

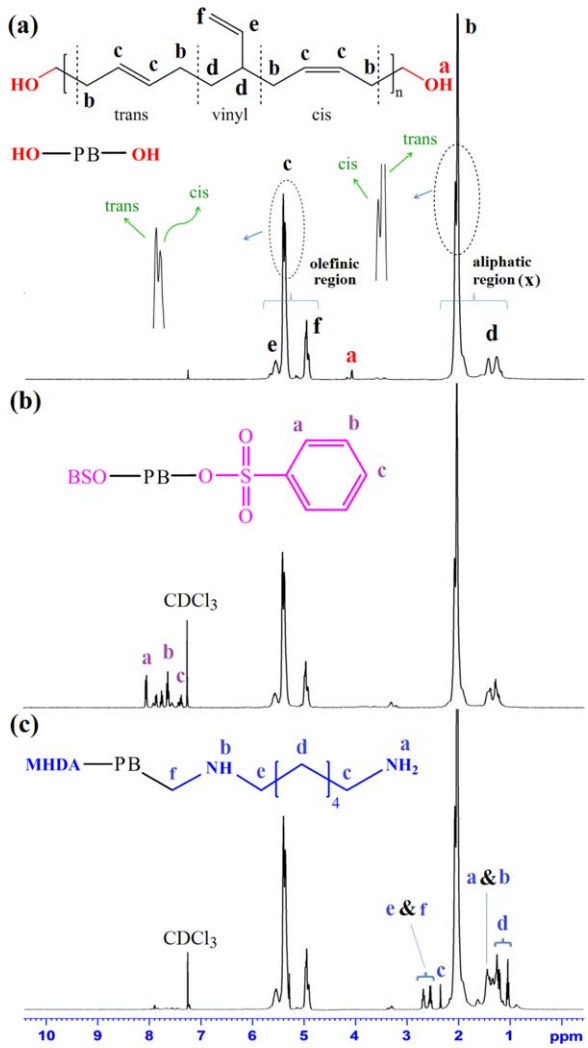


**Figure 3.** $^{1}$H NMR spectra for (a) HTPB, (b) intermediate, and (c) ATPB. [Color figure can be viewed in the online issue, which is available at wileyonlinelibrary.com.]

calculation of unsaturation degree by NMR data indicates that designed process in this work did not have undesirable effect on HTPB without using inhibitor.

### Mechanical Properties

The fracture toughness, flexural, and tensile tests were carried out in order to investigate the mechanical properties of the epoxy system modified with HTPB and ATPB liquid rubbers. The fracture toughness, flexural, and tensile properties of the cured ER specimens containing different amounts of the HTPB and ATPB are tabulated in Table I.

The stress–strain curves of the neat epoxy resin in addition to other specimens such as ERH5, ERH10, ERH15, ERA5, ERA10, and ERA15 are shown in Figure 4. The moduli of the rubber-modified specimens are lower than that of the neat epoxy. The similar effect was reported on other liquid rubber-modified epoxy systems such as HTPB,[25] CTBN,[26] and amine-terminated butadiene acrylonitrile (ATBN)[27] (e.g., the modulus decreases from 2.45 to 1.55 GPa by the addition of 15 phr aromatic ATPB rubber to epoxy resin).[21] Totally, it could be attributed to the low modulus of the rubbers. It seems that the effect of the rubber content on the reduction of Young's modulus is different in two ERH and ERA series of samples. As the rubber content increased from 5 to 10 phr, the tensile modulus decreased as much as 41 MPa (i.e., reduced from 1.73 to 1.69 GPa) for HTPB-modified samples with more pronounced reduction for the ATPB-modified which was 161 MPa (i.e., decreased from 1.70 to 1.54 GPa). The difference in modulus and the other characteristics (according to the data in Table I) could be due to this issue that in ATPB-modified epoxy; the rubber chains affect the properties more strongly since of possible chemical reaction of individual aminated chain in epoxy network.

The reduction in tensile and flexural strength could be related to two phase structure of the HTPB-modified network. Due to insufficient interaction of the rubber particles with epoxy matrix, the presence of rubber particles acts as a weak point and the rubber phase is the place for stress concentration. Additionally, the rubber is eligible to lower the crosslinking density of the network.[28] Thus, these phenomena led to the reduction of tensile and flexural strength in samples containing HTPB. Nonetheless, ATPB-modified samples showed a different trend. In the epoxy matrix modified with ATPB, the tensile strength did not experience sharp decrease when the rubber content was in the range of 5–10 phr; however, the flexural strength decreased in comparison with the neat epoxy network. Similar observations on tensile strength were reported by incorporation of other flexible diamines in the epoxy network.[29,30] It is well known that the internal stress produced in epoxy resins during curing process. The internal stress within the bulk material is able to influence the performance of the final product

**Table I.** Mechanical Properties of Different HTPB and ATPB-Modified Epoxy Networks

| Sample code | Tensile strength (MPa) | Young's modulus (GPa) | Elongation at break (%) | Flexural strength (MPa) | Flexural modulus (GPa) | KIC (MPa m1/2) | GIC (kJ $m^{-2}$) |
|---|---|---|---|---|---|---|---|
| ER | 70.3 ± 3.4 | 1.87 ± 0.02 | 4.5 ± 0.34 | 88.9 ± 1.2 | 2.63 ± 0.08 | 0.85 ± 0.15 | 0.38 ± 0.22 |
| ERH5 | 65.9 ± 3.2 | 1.73 ± 0.04 | 4.9 ± 0.38 | 78.7 ± 0.8 | 2.32 ± 0.06 | 1.53 ± 0.22 | 1.35 ± 0.33 |
| ERH10 | 61.3 ± 1.5 | 1.69 ± 0.02 | 5.1 ± 0.45 | 69.8 ± 2.3 | 2.05 ± 0.14 | 1.80 ± 0.19 | 1.92 ± 0.28 |
| ERH15 | 50.7 ± 2.4 | 1.61 ± 0.03 | 5.2 ± 0.44 | 64.3 ± 1.4 | 1.94 ± 0.05 | 1.32 ± 0.20 | 1.08 ± 0.30 |
| ERA5 | 76.0 ± 2.1 | 1.70 ± 0.03 | 5.5 ± 0.51 | 85.4 ± 1.7 | 2.14 ± 0.10 | 1.71 ± 0.25 | 1.72 ± 0.49 |
| ERA10 | 72.5 ± 3.2 | 1.54 ± 0.01 | 7.8 ± 0.58 | 81.0 ± 2.5 | 1.97 ± 0.07 | 2.16 ± 0.22 | 3.02 ± 0.43 |
| ERA15 | 48.7 ± 4.0 | 1.43 ± 0.04 | 10.4 ± 0.62 | 68.4 ± 2.1 | 1.64 ± 0.12 | 1.26 ± 0.20 | 1.11 ± 0.37 |

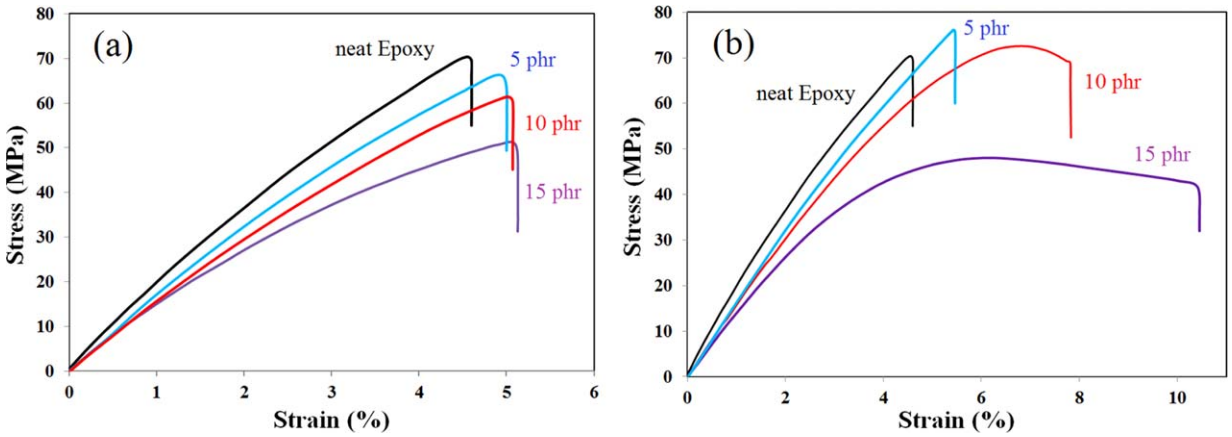


**Figure 4.** Stress–strain curves of unmodified and modified epoxy resins with different contents of (a) HTPB and (b) ATPB. [Color figure can be viewed in the online issue, which is available at wileyonlinelibrary.com.]

significantly through creating micro-cracks andvoids.[31] On the contrary, the introduction of soft segments into brittle epoxy resins can drastically decrease the internal stress. Thus, the increase in the strength by including suitable amounts of flexible diamines could be due to the reduction of internal stress in the samples in the presence of soft segment into the brittle epoxy network. The rubber which is incorporated into the matrix is responsible for the reduction in flexural strength of the modified samples. Prior works on rubber-modified epoxies are in agreement with this observation.[19,28]

The variation in the values of fracture toughness (critical stress intensity factor, $K_{1C}$) and fracture energy (critical strain energy release rate, $G_{1C}$) as a function of rubber content is demonstrated in Figure 5. The addition of rubber imparts an increase in the value of $K_{1C}$ up to an optimum rubber content of 10 phr, and it is notable that fracture energy also shows the same trend. No further increase was observed on further loading of rubber. In HTPB/epoxy system, the toughness improvement is attributed to rubber particles that enhance shear localization by acting as stress concentrators. While in the case of toughened

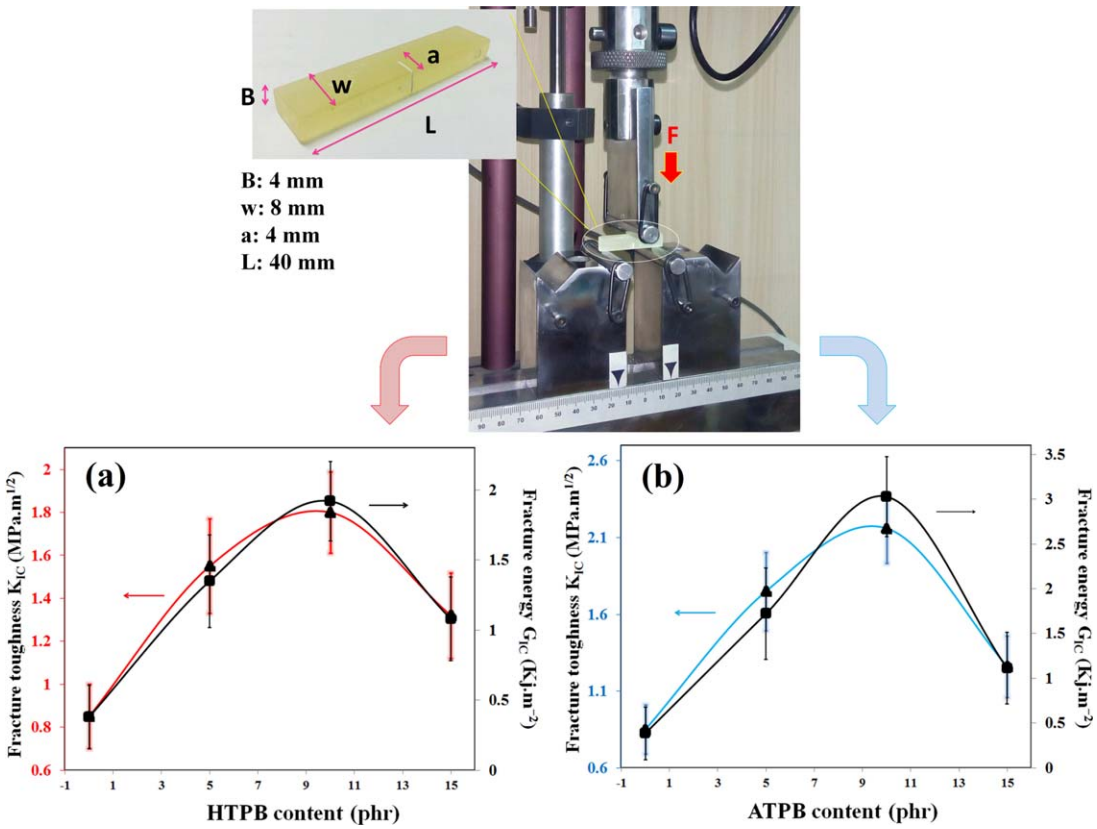


**Figure 5.** Fracture toughness and fracture energy as a function of (a) HTPB and (b) ATPB contents. [Color figure can be viewed in the online issue, which is available at wileyonlinelibrary.com.]

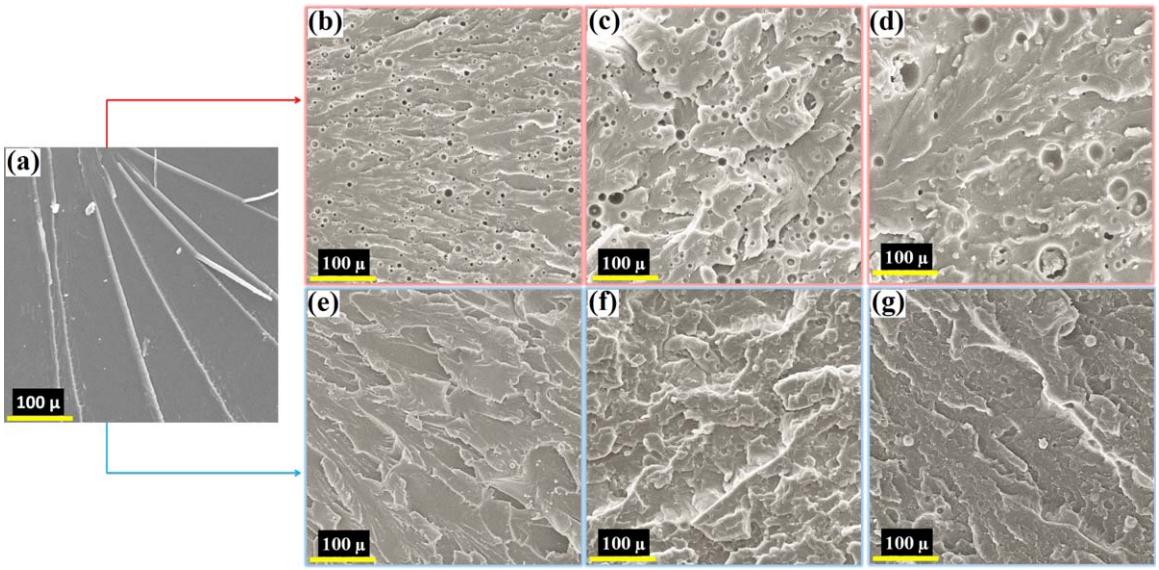


**Figure 6.** SEM micrographs of the fractured surface of unmodified and modified epoxy resins. (a) Unmodified epoxy; (b) 5 phr HTPB; (c) 10 phr HTPB; (d) 15 phr HTPB; (e) 5 phr ATPB; (f) 10 phr ATPB; and (g) 15 phr ATPB. [Color figure can be viewed in the online issue, which is available at wileyonlinelibrary.com.]

samples with ATPB, the rubber chains that are chemically bonded to the matrix can tolerate the load in tri-axial tension. Hence, ATPB as a flexible diamine is able to induce flexibility to epoxy network. This effect enhances ability of the matrix to deform under shear. Since the addition of every part of the amine-terminated liquid rubber causes a dramatic increase in the number of rubber chains in epoxy network; therefore, this influences the whole system. This is, perhaps, the reason for the high increase of $K_{1C}$ values with ATPB loading that be effective than HTPB (with 10 phr of ATPB and HTPB, $K_{1C}$ is equal to 2.16 and 1.80 MPa $m^{1/2}$, respectively). Moreover, the toughness enhancement is thought to be attributed to the increase in main chain mobility and degree of entanglement between the resin and the rubber.

The trend of fracture toughness attributing to the HTPB-modified epoxies is in agreement with the previous reports.[28,32] It is worthy to note that, in comparison with toughness modification,[27,28,33] the increase in the value of the toughness was not only significantly high, but also the ATPB toughened the epoxy resins without sacrificing the tensile strength. Fellahi *et al.*[27] reported that by using of ATBN that could toughen epoxy matrix, the value of $K_{1C}$ increased from 0.91 to 1.49 MPa $m^{1/2}$. In the present work, the amount of $K_{1C}$ increased from 0.85 to 2.16 MPa $m^{1/2}$. Therefore, it can be claimed that the ATPB provides higher toughness for epoxies. One of the reasons (in addition to structural differences) is number of amines in the structure of ATPB (four amines per chain) that could create stronger bonds with epoxy network. Therefore, stress can be transferred more efficiently, and as a result, higher toughness is achievable.[17,27]

The differences in mechanical behavior of the samples could be further associated with morphological investigations. Microscopic techniques were used to describe an appropriate explanation for the variation of mechanical properties. This task will be discussed in the following sections.

### Morphological Studies

Morphology characterization using SEM images plays a vital role in the establishment of the structure–property relationship. Representative microscopic images of the fractured surfaces of the neat and modified epoxies are depicted in Figure 6. The SEM micrograph of the unmodified epoxy in Figure 6(a) shows a river plot, smooth, and glassy fractured surface with cracks in different planes. This observation indicates brittle fracture of the network, which is a proof to its poor fracture toughness, as there is no significant energy dissipation mechanism operating and plastic deformation here.

The fractured surface of the HTPB/epoxy systems, Figure 6(b–d) (representing 5–15 phr rubber content), obviously suggests two distinct phases; a rigid continuous epoxy matrix and a dispersed rubbery phase of isolated spherical particles. This heterogeneous morphology led to opacity in samples. The holes visible in the SEM micrographs are due to the particles that are extracted from the surface of the samples after treatment with toluene. The SEM micrographs of the toughened epoxy networks containing 5, 10, and 15 phr of ATPB are shown in Figure 6(e–g). These modified epoxy networks are visually homogeneous, showing a single-phase system. This may be attributed to the incorporation of the rubber chains into epoxy matrix through chemical reactions of ATPB chains with epoxy resin. Consequently, the rubber domains are not observable by SEM. Figure 7 suggests the schematic diagrams for morphological evolution of the HTPB/epoxy and ATPB/epoxy systems. The chain extension of the ATPB/epoxy system maybe made possible by the chemical reaction between amine end groups of the ATPB and epoxy ring which was confirmed by FTIR spectroscopy.

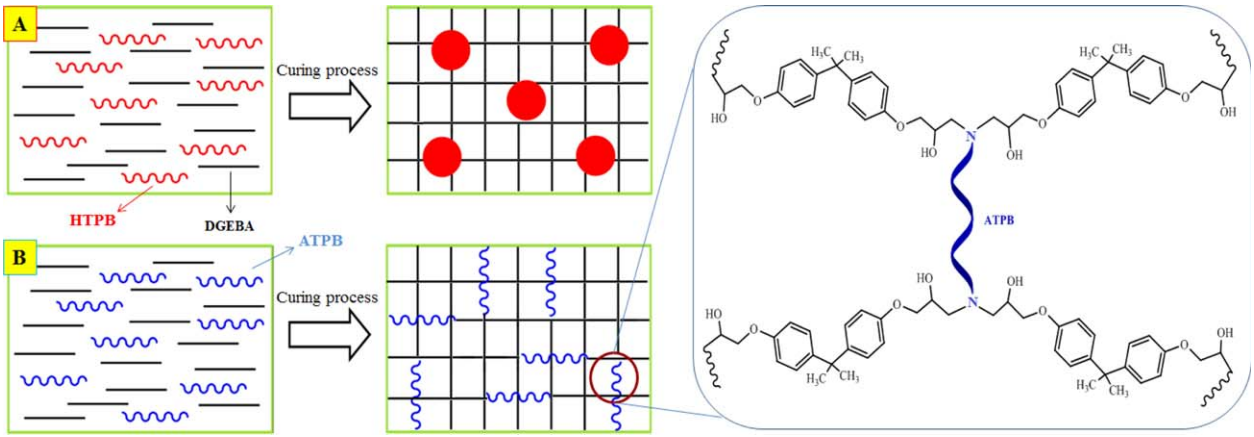


**Figure 7.** Schematic diagrams for morphology evolution of (A) the traditional HTPB/epoxy composite and (B) the chemically modified epoxy system with ATPB in the process of curing. [Color figure can be viewed in the online issue, which is available at wileyonlinelibrary.com.]

**Fractography of HTPB/Epoxy System.** In epoxies containing 5 and 10 phr of HTPB, which were shown in Figure 6(b,c), respectively, the rubber particles are uniformly distributed throughout the epoxy matrix, whereas the sample containing 15 phr of rubber content showed a heterogeneous distribution of particles as observed in Figure 6(d). According to the histogram attained from SEM images analysis in Figure 8, the size of the precipitated rubbery domains enhances with the increase in rubber content of the formulations. Besides, the number and volume average of the domains are found to be increased with respect to rubber content, which is in agreement with the behavior of other rubber-modified epoxies.[18,34,35] Moreover, the distribution of particle size in ERH5 is broad and the addition of the rubber to 10 phr resulted to the narrow size distribution. However, in the ERH15 sample a larger particle size and broader particle size distribution than others are observed. It was shown that interparticle distance increases with higher incorporation of rubber implying for less interactions of rubber particles with epoxy matrix.[28] Thus, there is a possibility of coalescence of some rubber particles in the sample with low rubber content (i.e., sample ERH5) due to the low interparticle distance and low viscosity of the HTPB. It perhaps led to broadening of the size distribution. On the other hand, in the sample with high rubber (i.e., sample ERH15), some particles probably could not approach each other in coalescence process during curing due to the high inter-particle distance. Therefore, the size distribution was broader for sample ERH15 compared to other samples. The study of the particles size and distribution in addition to dispersion and distance from each other suggests valuable suggestions in mechanical properties. This relation between properties and morphology could be elaborated *via* fracture mechanisms.

The main mechanisms of inelastic deformation in rubber-toughened plastics (and in other identical multiphase systems) are: yielding process in the rigid phase (e.g., epoxy matrix) and cavitation in the soft dispersed phase (e.g., HTPB).[36,37] The unimodal distribution of isodiametric rubber particles is estimated to be responsible for lower crack growth in ERH10 specimen, and that could be indicated by the presence of relatively large number of deformation lines in its micrograph. As it can be seen in Figure 6(c), the deformation lines are propagated through rubber domains, which facilitate stress transfer between the particles and epoxy matrix. Therefore, Figure 6(c) indicates the yielding process operating throughout the matrix. Additionally, the micrograph of ERH10 shows stress-whitened zone of broken rubber particles that was resulted from voids developed in the matrix due to cavitation of rubber particles. These mechanisms have been explained by researchers as the most critical

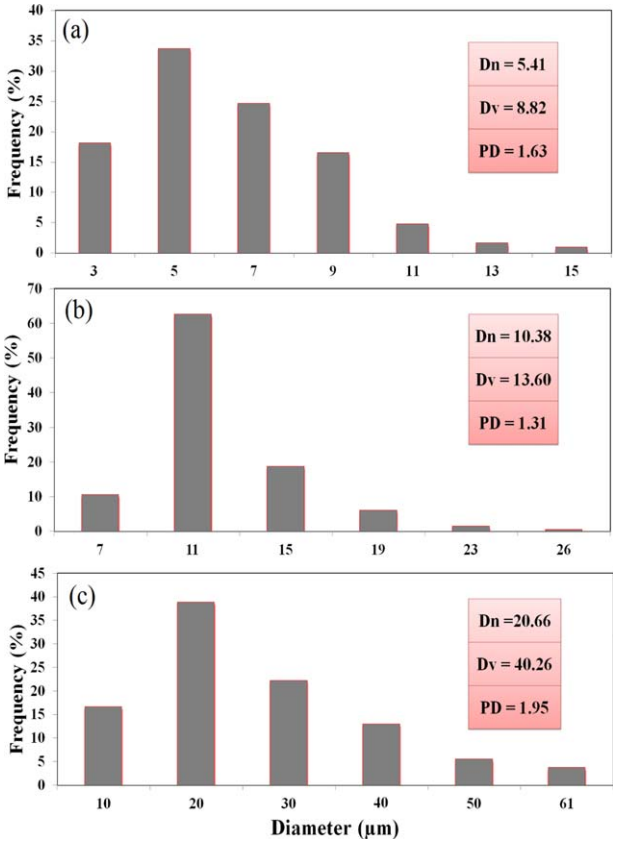


**Figure 8.** Particle size distribution in (a) 5 phr, (b) 10 phr, and (c) 15 phr HTPB-modified epoxy systems. [Color figure can be viewed in the online issue, which is available at wileyonlinelibrary.com.]

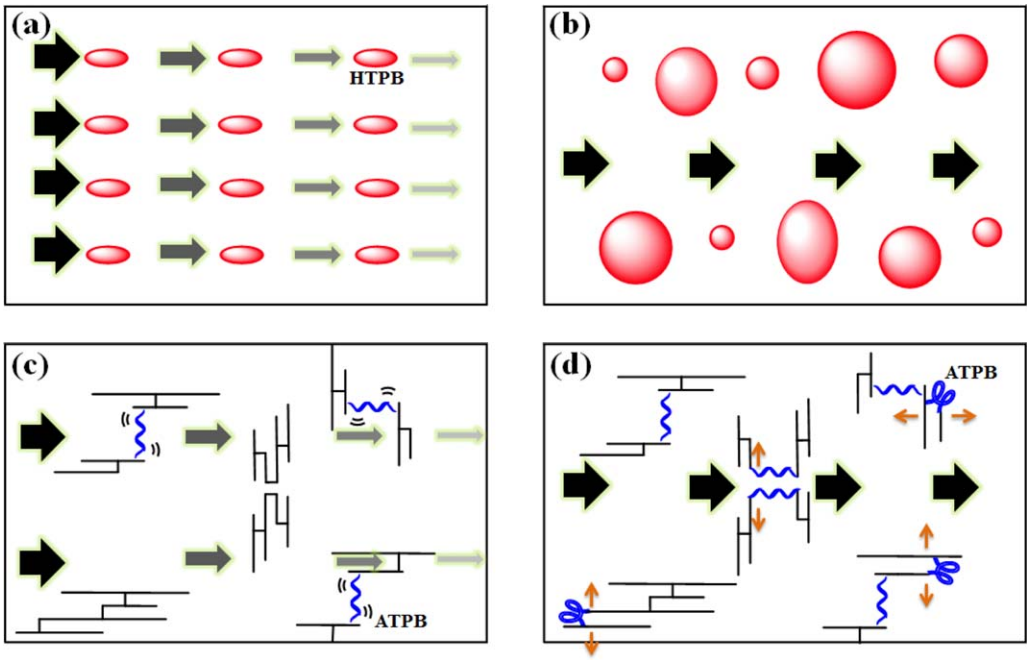


**Figure 9.** Schematic representation of the energy dissipation mechanism in the modified epoxy with: (a) lower content of HTPB, (b) higher content of HTPB, (c) lower content of ATPB, and (d) higher content of ATPB. [Color figure can be viewed in the online issue, which is available at wileyonlinelibrary.com.]

energy dissipation mechanisms acting in rubber-modified epoxies.[36,37] The morphological structure of sample ERH10 appeared to be responsible for the highest fracture toughness of modified epoxies. Even though the particle distribution is homogenous in the sample ERH5, but the mechanical property has become weaker than ERH10. The lower mechanical properties maybe attributed to the absence of a uniform particle size distribution and lack of the similar distance between particles as observed in fractured surface. In higher weight percentage of rubber-modified sample, a heterogeneous particle size distribution, non-uniform distribution of particles, bigger particles and nonidentical interparticle distance is observed for sample ERH15 in Figure 6(d). As a result, the poor mechanical performance of epoxy systems with high content of liquid rubber could be attributed to this undesirable morphological structure.

The homogeneous distribution of isodiametric elastomer particles act as stress concentrators in epoxy systems with lower weight percentage of rubber. As the force is applied; the energy transfer occurs through particles and also dissipates in the network. Hence, the matrix is maintained from a severe failure. As it is depicted in Figure 9(a), the spherical shapes represent the elastomeric particles in the epoxy matrix. The arrow indicates the crack energy propagation. The crack energy propagation gradually reduces as it passes through elastomeric particles. The dissipation of energy is illustrated by the decrease in size and color intensity of the arrow. The small pale arrow demonstrates that the initial energy is decreased as it passes through rubber particles. There occurs a distortion in particles as it propagates energy, but this is not represented in the figure. As observed in Figure 6(c), this phenomenon protects the sample against fracture by creating the wrinkle plot of the fractured surface.

Figure 9(b) illustrates that the modified epoxy with higher content of rubber is characterized by elastomeric particles with larger sizes and less regular distribution. The arrows suggest crack propagation through the interface. There is no reduction in the crack energy intensity as it is not propagated through elastomer particles, which is denoted by the same style of arrows. This causes interfacial separation which leads to failure of the matrix. This phenomenon is clearly sensible in micrograph of the ERH15 [Figure 6(d)], which permits the crack growth between rubber phases. To achieve benefit from a shear yielding mechanism, the rubber particles should interact with the crack tip.[38] Therefore, the chance of shear yielding mechanism in this sample is low which resulted in the lowest fracture toughness.

**Fractography of ATPB/Epoxy System.** The SEM micrographs of the epoxy networks containing 5, 10, and 15 phr of ATPB [Figure 6(e–g), respectively] show that the fractured surfaces of ATPB-modified epoxies, unlike neat epoxy, are not very smooth. This observation indicates the ductile manner of fracture. According to Yee and Pearson,[39] the size of stress-whitened zone or amount of deformation lines is proportional to the increase in toughness. In the case of the ERA10 specimen, which is shown in Figure 6(f), high roughness was observed that could be due to the significant plastic deformation at the crack tip. The relatively brittle fractured surface in the micrograph of the ERA15 [see Figure 6(g)] demonstrates that this sample has lower toughness than samples ERA5 and ERA10.

Figure 9(c,d) shows schematic of the crack propagation and energy dissipation for ATPB-modified epoxy. Same as the previous schematic, the arrows represent the crack energy propagation. In the modification of epoxy network by polybutadiene

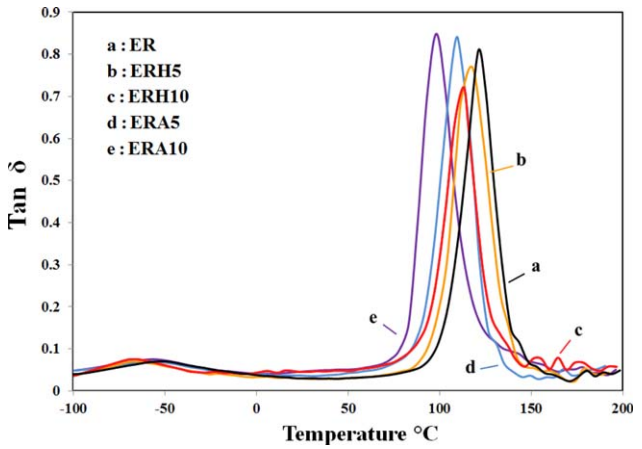


**Figure 10.** Loss factor (tan δ) curves of (a) neat epoxy, (b) HTPB (5 phr)/epoxy, (c) HTPB (10 phr)/epoxy, (d) ATPB (5 phr)/epoxy, and (e) ATPB (10 phr)/epoxy systems. [Color figure can be viewed in the online issue, which is available at wileyonlinelibrary.com.]

polyamine, ATPB is replaced instead of DETA so that a flexible structure takes the place of the curing agent. This variation in epoxy network architecture makes the nature of the sample to be changed and demonstrates a tough behavior against applying stress. Therefore, while the material undergoes fracture, crack is propagated through the network by an energy dissipation mechanism and this is due to the damping nature of the toughened epoxy caused by flexible backbone of the ATPB [as seen in Figure 9(c)]. Hence, the micrograph related to the fractured surfaces of the modified samples, shows a tough surface. This attitude, appears more by the enhancement of the rubber content; so that the micrograph surface of the sample ERA10 suggests more tough and rough surface in comparison to ERA5; while the addition of 15 phr of ATPB to epoxy system leads to the observation of relatively a smooth surface in the micrograph. The reason behind this issue could be of two factors including the decrease in crosslinking density (confirmed by DMA results in the next part) and the high reduction in cohesive energy. Even though DETA is replaced with ATPB in the ATPB/epoxy system, because of the existing distance between two crosslink sites in the sample containing ATPB, the crosslinking density decreases. On the other hand, the chemical bonds form between the amine groups of the ATPB and epoxy groups. However, the lack of effective interactions between the polybutadiene backbone and epoxy network may result to lower cohesive energy. Thus, the fracture trend is recommended in Figure 9(d). The crack propagation is carried out with a low energy amount and the breakage occurs with a low crack energy loss.

### Dynamic Mechanical Properties

The dynamic mechanical behaviors of neat epoxy and the rubber-modified epoxy systems were measured to achieve more insight into the observed toughening effect. The loss factor (tan δ) versus temperature curves for neat and rubber-modified epoxies are depicted in Figure 10.

Two relaxation zones for all the epoxy systems are discernible from loss factor (tan δ) curves. In the tan δ curve of the neat epoxy, a peak at about 121 °C is observed indicating for the glass transition temperature ($T_g$) of epoxy resin. This primary relaxation phenomenon known as α relaxation is attributed to the macromolecular chain movements. The tan δ curve of the unmodified epoxy also showed a broad and a less intense peak at a lower temperature range (near −50 °C). The low temperature tan δ peak refers to the sub-glassy relaxation process which is nominated as β relaxation of epoxy resin. This transition could be due to the crankshaft motion of the glyceryl-like groups in DGEBA.[40]

The peak related to $T_g$ was slightly shifted to the lower regions through the addition of the HTPB rubber to the epoxy resin. In fact, by the addition of 5 and 10 phr of HTPB rubber, the displacement to the lower temperatures would be 3 and 8 °C, respectively. This might be attributed to the decrease in crosslinking density in the rubber modified samples. During epoxy resin curing, the phase separated rubber domains would fill and occupy some spaces through the reacting sites, hence, the crosslinking reaction would be impaired and subsequently the crosslinking density of the modified systems shall be reduced. Therefore, the total crosslinking density changes by the incorporation of more HTPB rubber. There are similar results supporting this finding which have been reported before.[19,26,28]

In the case of the ATPB-modified epoxy, by an increase in the weight fraction of the ATPB liquid rubber, the $T_g$ decreases to the lower temperatures. It is due to this fact, that by the addition of polybutadiene polyamine to the epoxy system, rubber chains as flexible segments are incorporated into the network as proved previously with the FTIR results. Also, because of the easier mobility of the rubbers compared to epoxy resin, the $T_g$ decreases more than a HTPB/epoxy system. As it is shown in Figure 7, the ATPB rubbers compose rubber moieties and lead to more network flexibility. The addition of flexible modifier often causes a decrease in the $T_g$ which is attributed to introduction of a structure with low $T_g$ in the epoxy network by chemical reaction between the flexible phase and the rigid epoxy resin.[27] Zhang *et al.*[41] reported the urea-terminated polybutadiene-modified epoxy system that the $T_g$ falls from 160.6 to 104.3 °C using 10 phr of liquid rubber, which is unambiguously due to the flexibility of polybutadiene. However, in the present study, as prepared ATPB caused intensive increase in fracture toughness comparing to other liquid rubbers[28,33] and flexible diamines[27,31] that led to negligible decrease in $T_g$.

The variations of the storage modulus for the samples are represented in Figure 11. As observed, the storage modulus of the samples decreased when the rubber was added. Investigation of values of the storage modulus at lower $T_g$ zone (at 25 °C) showed the same trend as the elastic modulus resulted from mechanical testing. As it is illustrated in Figure 11, there is a loss in storage modulus in the rubbery plateau region through addition of the indivitual rubber phase, that is, HTPB and ATPB. Besides, the higher content of the rubber, the lower the stiffness of the epoxy would be. Based on the rubber elasticity theory, the plateau of storage modulus at temperatures above $T_g$ is proportional to crosslink density.[26] Therefore, it could be deduced from decrease in the rubbery plateau region that the

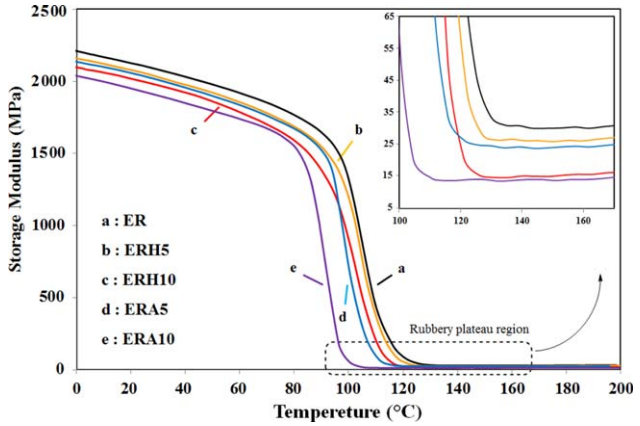


**Figure 11.** Storage modulus versus temperature curves for the neat epoxy resin in addition to different rubber-modified epoxy resins. [Color figure can be viewed in the online issue, which is available at wileyonlinelibrary.com.]

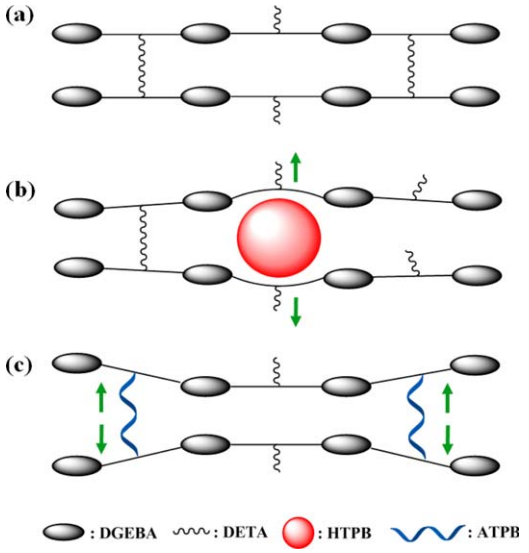


**Figure 12.** Schematic representation of curing network structures of (a) unmodified, (b) HTPB-modified, and (c) ATPB-modified epoxy resin systems. [Color figure can be viewed in the online issue, which is available at wileyonlinelibrary.com.]

presence of the liquid HTPB rubber may reduce the crosslink density at interface of the modified epoxy resins. In the ATPB-modified epoxies, if the rubber actually dissolves into the matrix without interfering with network formation, one would expect little change in modulus.[42] On the other hand, if added rubber reacts with the epoxy matrix through terminal amine groups, the modulus should decrease due to the loosening of network. Since, the relative modulus sharply dropped, it is indirect evidence that the rubber reacted with the epoxy resin. Consequently, the relatively sharp drop of modulus in this system shows that ATPB had a higher influence on decrease in crosslinking density than HTPB through reaction with epoxy. Furthermore, it has been proposed that the decrease in the crosslinking density is likely to be the main reason for the fracture toughness improvement.[43,44] Thus, to investigate more precisely, the molecular weight between two crosslinks ($M_c$) and crosslinking density resulted from this test was studied.

The rubbery plateau region of the DMA spectrum could be yields valuable information about the $M_c$ of the network systems. Thus, $M_c$ of the epoxy networks was evaluated from DMA results, using the equation based on rubber-like elasticity. According to the rubber elasticity theory, the $M_c$ of a network can be obtained using the following equation[45]:

$$M_c = \frac{3\rho RT}{E'} = \frac{\rho}{\nu} \quad (8)$$

where $E'$ is the storage modulus at $T_g + 30\,^{\circ}C$, $R$ is the universal gas constant, and $T$ is the absolute temperature at $T_g + 30\,^{\circ}C$. Also, ρ is the density of the samples, which was determined by KERN densitometer. $\nu$ is the crosslinking density of the epoxy networks which is inversely related to $M_c$ and is equal to $E'/3RT$.[43] It is worth to be noted that the above equation is achieved from the rubber elasticity theory for rubbers but in this study, the rubbery plateau modulus of the samples was used instead of the storage modulus. The calculated amounts are shown in Table II.

As it is shown in Table II, by the addition of the rubber (both HTPB and ATPB), the amount of $\nu$ decreases and $M_c$ increases. For explicit specification, schematic illustration of the epoxy network crosslinking of neat and two modified forms of the epoxy systems (i.e., HTPB/epoxy and ATPB/epoxy) is shown in Figure 12(a–c), respectively. The decrease in the amount of $\nu$ for the samples with 5 and 10 phr of HTPB could be due to this fact that the phase separated domains occupy the space between reaction sites [as seen in Figure 12(b)]. Therefore, this causes enhancement in space between these sites and also reduction in the amount of crosslinking sites and eventually the crosslinking density would be decreased. In the case of the samples modified with ATPB rubber, the reason behind the decrease of ν is that by addition of ATPB, the end amine groups would react with epoxy chains and act as a crosslinking agent. As can

**Table II.** DMA Results of the Neat and Rubber-Modified Epoxy Resins

| Sample code | $T_g$ (°C) | $E'$ (MPa)[a] | $\rho$ (g cm$^{-3}$) | ν ($10^{-3}$ mol cm$^{-3}$) | $M_c$ (g mol$^{-1}$) |
|---|---|---|---|---|---|
| Epoxy resin (ER) | 121 | 30 | 1.1813 | 2.75 | 425.26 |
| ER + HTPB5 | 118 | 26 | 1.1633 | 2.41 | 477.63 |
| ER + HTPB10 | 113 | 15 | 1.1426 | 1.47 | 803.66 |
| ER + ATPB5 | 110 | 24 | 1.1603 | 2.31 | 512.48 |
| ER + ATPB10 | 98 | 14 | 1.1405 | 1.42 | 849.33 |

[a] At $T_g + 30\,^{\circ}C$.

be seen in Figure 12(c), due to the longer chains of ATPB compared to DETA, distance between the sites and epoxy chains increases and consequently the crosslinking density drops down. Comparsion of the $M_c$ and $v$ values of two series of these samples (i.e., HTPB and ATPB-modified epoxies) indicates that incorporation of the ATPB is more effective than HTPB on the structural properties of the epoxy network. Besides, according to the pattern of changes in the aforementioned amounts and comparing them to the pattern resulted from the mechanical properties, the close relation between structure and properties is observed. From these results, it is concluded that the toughening effect of ATPB originates from change in architecture of the epoxy system that significantly different from dispersed HTPB particles system.

## CONCLUSIONS

The reactive ATPB was successfully prepared via amination of the HTPB and subsequently incorporated in an epoxy system. The FTIR characterization showed chemical reactivity of the ATPB at mild condition. It is worth to note that the tensile strength of the chemically modified epoxy resin with ATPB is higher than that of neat epoxy, whereas Young's modulus decreases moderately with increasing ATPB content. The fracture toughness of the ATPB-modified epoxy resin was dramatically improved in comparison with HTPB-modified epoxy. In comparison with that of neat epoxy, the sample with 10 phr ATPB suggested a significant enhancement of $K_{IC}$ and $G_{IC}$ from 0.85 to 2.16 MPa $m^{1/2}$ and from 0.38 to 3.02 kJ $m^{-2}$, respectively. The toughening effect of the ATPB on the epoxy system was further confirmed by microscopic observations of the fractured surfaces. The SEM observations showed that the toughening effect in ATPB-modified epoxy originates from the difference in architecture between ATPB and epoxy network unlike those from dispersed HTPB particles. According to the results of mechanical and DMA, the toughening effects are considered to arise mainly from the incorporation of flexible diamines in the epoxy network and lower crosslinking density. Generally, this work opens up the possibility of utilizing high reactive polyamines with flexible polybutadiene backbone as effective toughening agents for epoxies.

## REFERENCES


1. Kishi, H.; Tanaka, S.; Nakashima, Y.; Saruwatari, T. *Polymer* **2016**, *82*, 93.
2. Abdollahi, H.; Ershad-Langroudi, A.; Salimi, A.; Rahimi, A. *Ind. Eng. Chem. Res.* **2014**, *53*, 10858.
3. Zhang, Z.; Tan, Y.; Wang, X.; Lin, Y.; Wang, L. *J. Appl. Polym. Sci.* **2016**, *133*, DOI: 10.1002/app.43500.
4. Yiying, Y.; Guo-Quan, L.; Boroyevich, D.; Ngo, K. D. T. *IEEE Trans. Components, Pack. Manuf. Technol.* **2015**, *5*, 168.
5. Barua, S.; Chattopadhyay, P.; Karak, N. *J. Mater. Chem. B* **2015**, *3*, 5877.
6. Sprenger, S. *Polymer* **2013**, *54*, 4790.
7. Abdollahi, H.; Salimi, A.; Maghsodian, S. *Basparesh* **2015**, *5*, 72.
8. Deng, S.; Djukic, L.; Paton, R.; Ye, L. *Compos. A: Appl. Sci. Manuf.* **2015**, *68*, 121.
9. Liu, T.; Nie, Y.; Zhang, L.; Chen, R.; Meng, Y.; Li, X. *RSC Adv.* **2015**, *5*, 3408.
10. Lou, C.; Zhang, X.; Wang, Y.; Chen, Z.; Li, H. *J. Appl. Polym. Sci.* **2015**, *132*, DOI: 10.1002/app.41345.
11. Iyer, K. A.; Torkelson, J. M. *Polymer* **2015**, *68*, 147.
12. Jin, F. L.; Liu, H. C.; Yang, B.; Park, S. J. *J. Ind. Eng. Chem.* **2015**, *24*, 20.
13. Jogi, B. F.; Kulkarni, M.; Brahmankar, P.; Ratna, D. *Procedia Mater. Sci.* **2014**, *5*, 787.
14. Zhou, H.; Xu, S. *Mater. Lett.* **2014**, *121*, 238.
15. Tripathi, G.; Srivastava, D. *Mater. Sci. Eng. A* **2007**, *443*, 262.
16. Kar, S.; Gupta, D.; Banthia, A.; Ratna, D. *Polym. Int.* **2003**, *52*, 1332.
17. Ramos, V. D.; da Costa, H. M.; Soares, V. L. P.; Nascimento, R. S. V. *Polym. Test.* **2005**, *24*, 387.
18. Mathew, V. S.; George, S. C.; Parameswaranpillai, J.; Thomas, S. *J. Appl. Polym. Sci.* **2014**, *131*, DOI: 10.1002/app.39906.
19. Barcia, F. L.; Amaral, T. P.; Soares, B. G. *Polymer* **2003**, *44*, 5811.
20. Chao, H.; Tian, N.; Drexler, A.; Schmidhauser, J. U.S. Patent 6,831,136 (**2004**).
21. Kar, S.; Banthia, A. K. *J. Appl. Polym. Sci.* **2005**, *96*, 2446.
22. Lee, H.; Neville, K. Handbook of Epoxy Resins; McGraw-Hill: New York, **1967**.
23. Pavia, D. L.; Lampman, G. M.; Kriz, G. S.; Vyvyan, J. R. Introduction to Spectroscopy, 4th ed.; Cengage Learning, Washington, DC, **2009**.
24. Ziaee, F. *Iran. J. Polym. Sci. Technol.* **2012**, *24*, 403.
25. Zhou, W.; Cai, J. *J. Appl. Polym. Sci.* **2012**, *124*, 4346.
26. Chonkaew, W.; Sombatsompop, N. *J. Appl. Polym. Sci.* **2012**, *125*, 361.
27. Chikhi, N.; Fellahi, S.; Bakar, M. *Eur. Polym. J.* **2002**, *38*, 251.
28. Thomas, R.; Yumei, D.; Yuelong, H.; Le, Y.; Moldenaers, P.; Weimin, Y.; Czigany, T.; Thomas, S. *Polymer* **2008**, *49*, 278.
29. Strzelec, K.; Leśniak, E.; Janowska, G. *Polym. Int.* **2005**, *54*, 1337.
30. Feng, Q.; Yang, J.; Liu, Y.; Xiao, H.; Fu, S. *J. Mater. Sci. Technol.* **2014**, *30*, 90.
31. Yang, G.; Fu, S. Y.; Yang, J. P. *Polymer* **2007**, *48*, 302.
32. Thomas, R.; Ronkay, F.; Czigany, T.; Cvelbac, U.; Mozetic, M.; Thomas, R.; Ronkay, F.; Czigany, T.; Cvelbac, U.; Mozetic, M. *J. Adhes. Sci. Technol.* **2011**, *25*, 1747.
33. Wang, F.; Drzal, L. T.; Qin, Y.; Huang, Z. *Compos. A: Appl. Sci. Manuf.* **2016**, *87*, 10.
34. Mathew, V. S.; Sinturel, C.; George, S. C.; Thomas, S. *J. Mater. Sci.* **2010**, *45*, 1769.
35. Tang, L. C.; Wang, X.; Wan, Y. J.; Wu, L. B.; Jiang, J. X.; Lai, G. Q. *Mater. Chem. Phys.* **2013**, *141*, 333.

36. Bucknall, C. B. *J. Microsc.* **2001**, *201*, 221.

37. Gong, L. X.; Zhao, L.; Tang, L. C.; Liu, H. Y.; Mai, Y. W. *Compos. Sci. Technol.* **2015**, *121*, 104.

38. Bagheri, R.; Marouf, B. T.; Pearson, R. A. *Polym. Rev.* **2009**, *49*, 201.

39. Yee, A. F.; Pearson, R. A. *J. Mater. Sci.* **1986**, *21*, 2462.

40. Patil, P. N.; Rath, S. K.; Sharma, S. K.; Sudarshan, K.; Maheshwari, P.; Patri, M.; Praveen, S.; Khandelwal, P.; Pujari, P. K. *Soft Matter* **2013**, *9*, 3589.

41. Tian, X.; Geng, Y.; Yin, D.; Zhang, B.; Zhang, Y. *Polym. Test.* **2011**, *30*, 16.

42. Bussi, P.; Ishida, H. *J. Polym. Sci. B: Polym. Phys.* **1994**, *32*, 647.

43. Liu, W.; Zhou, R.; Goh, H. L. S.; Huang, S.; Lu, X. *ACS Appl. Mater. Interfaces* **2014**, *6*, 5810.

44. Kang, B. U.; Jho, J. Y.; Kim, J.; Lee, S. S.; Park, M.; Lim, S.; Choe, C. R. *J. Appl. Polym. Sci.* **2001**, *79*, 38.

45. Wu, T. H.; Foyet, A.; Kodentsov, A.; van der Ven, L. G. J.; van Benthem, R. A. T. M.; de With, G. *Mater. Chem. Phys.* **2014**, *145*, 342.